Dispersion Optimization in GeO_2-doped Silica Photonic Crystal Fibers with Circular Lattice

Thuy Nguyen Thi
University of Education, Hue University, 34 Le Loi, Hue City, Viet Nam.
Email: ntthuy@hueuni.edu.vn

Received: 13 January 2023 Revised: 9 February 2023 Accepted: 8 March 2023

ABSTRACT:
In this paper, we analyze the dispersion properties of photonic crystal fiber with the core replaced by a composite of 85% SiO_2-15% GeO_2. The air hole's radii of the layers in the cladding are designed differently to improve the dispersion and nonlinear properties of the fibers. Both anomalous and all-normal dispersions have been optimized. Based on numerical simulation results, two optimal structures (d_1/Λ = 0.4, Λ = 0.9 µm and d_1/Λ = 0.45 and Λ = 1.0 µm) are proposed with a very small dispersion value of 0.298 ps/ nm.km and −0.311 ps/nm.km at the pump wavelength of 1.53 µm and 0.985 µm, respectively. The high nonlinear coefficient, small effective mode area, and very low attenuation of about 10^{-7} dB/m at the pump wavelength are also favorable conditions for the application of broad-spectrum supercontinuum with low peak power. The proposed fibers can be new supercontinuum sources that effectively replace glass core fibers.

KEYWORDS: Photonic Crystal Fibers, Composite SiO_2-GeO_2, Flat Dispersion, Small Effective Mode Area, Low Attenuation.

1. INTRODUCTION

With its excellent nonlinear properties, Photonic Crystal Fiber (PCF) has verified wide applicability in fields including: optical coherence tomography, photonic device testing, optical communications [1]–[5], and optical microscopy [6], [7]. Furthermore, it is also the best nonlinear mediums for supercontinuum (SC) generation [8], due to its flexibility in structural design and high nonlinearity. Generally, silica-based solid-core PCFs are most commonly used to produce a broad SC with high intensity but it is difficult to extend the spectrum further in the mid-infrared region (MIR) due to silica's high matter absorption. To avoid this limitation of silica, many recent studies have suggested the development of broadband sources based on different optical mediums such as the hollow-core photonic crystal fibers which are infiltrated by highly nonlinear liquids [9]–[12], fibers made of fluoride [13]–[16] or chalcogenide [17]–[20]. Although the efficiency of SC spectrum expansion is improved in MIR, they are often expensive, fragile and rather difficult to handle. The physical properties of Germania (GeO_2) and silica (SiO_2) are similar but the phonon energy of GeO_2 (~820 cm^{-1}) is lower than of silica (~1100 cm^{-1}), its nonlinear refractive index (9.5×10^{-20} $m^2.W^{-1}$) is about 3.5 times higher than that of silica (2.74×10^{-20} $m^2.W^{-1}$). [21]. This makes the transmission window of GeO_2-based PCFs longer in MIR [22]. The high optical transparency of pure GeO_2 and GeO_2 doped silica fibers in the MIR is one of the advantages that attract the attention of the research groups. More, these PCFs have been fabricated in practice by drawing methods for silica fibers [23]. Recently, many publications have presented on SC spectral broadening in MIR based on GeO_2-doped core silica fibers [22], [23]–[28]. SC spectral expansion using GeO_2-doped silica fibers with different laser pump pulses at 1.5 µm and 2 µm have been also investigated in [29], [30]. In the experiment, some silica fibers have a GeO_2 doped core with concentrations varying from 51 mol% to 97 mol% [31]–[33], and low loss (less than 120 dB/km at 1.9–2 µm) have been reported. A broad spectrum from 700nm to 3200nm based on GeO_2-doped PCF at 1.55m pump wavelength was proved by the experiment in the work [34]. The papers [35, 36] showed that GeO_2-doped PCFs had been experimentally fabricated to obtain broad-spectrum SC at different pumping wavelengths although the damage threshold of GeO_2 is low (few orders of magnitude lower than that of silica) [37].

In this paper, we investigate in detail the specific quantities for dispersion and nonlinear properties of

Paper type: Research paper
DOI: 10.30486/mjee.2023.1977591.1057
How to cite this paper: T. Nguyen Thi, **"Dispersion Optimization in GeO2-doped Silica Photonic Crystal Fibers with Circular Lattice"**, *Majlesi Journal of Electrical Engineering*, Vol. 17, No. 2, pp. 59-67, 2023.

silica fibers doped GeO_2 with a concentration of 15% mol. All-normal and anomalous flat dispersions beneficial to SC generation are obtained. More, quantities such as effective mode area, nonlinear coefficient, and attenuation are also analyzed numerically and compared with previous publications on GeO_2-doped PCFs. Two optimized structures with flat dispersion, high nonlinear coefficient, and low attenuation are proposed to guide SC generation application.

2. NUMERICAL MODELLING OF PCFs

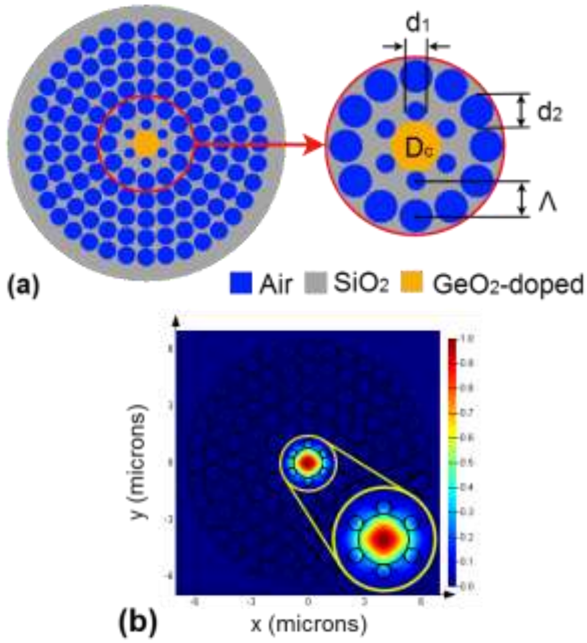

Fig. 1. Cross-section view of the circular GeO_2-doped silica PCF (a), and the light confinement in the core of PCF with Λ = 1.0 µm; d_1/Λ = 0.45 (b).

The structure and optical properties of GeO_2-doped silica PCF were simulated using Lumerical Mode Solution (LMS) software. The full-vector finite-difference eigenmode method is used to mesh waveguide geometry and is capable of fitting arbitrary waveguide structures. Once the structure is meshed, Maxwell's equations are then built into a matrix eigenvalue problem and solved using sparse matrix techniques to calculates the spatial profile and frequency dependence of modes. The boundary condition is the perfectly matched layers with rectangular shape which strongly absorbs the waves coming from the calculated region without any reflection. As a result, we obtain the effective refractive index, loss, and the field intensity profile of the fundamental mode of the PCFs. The cross-sectional structure of GeO_2-doped silica PCF is shown in Fig. 1a. Six layers of air holes with diameter d separated by a distance Λ are arranged in a circular pattern around the core. The works [9]–[11] verified that the dispersion was efficiently controlled by reasonably adjusting the air hole's size of the first layer near the core. Even the Zero Dispersion Wavelengths (ZDWs) shift is strongly affected by this. But the attenuation of the fundamental-mode or the higher order modes is dominated by the size of the remaining layers. From this idea, we modified the lattice structure which focused on the difference between the air hole's diameter of the layers in the cladding to control the dispersion and nonlinear properties of the fibers. The filling factor d_1/Λ varies from 0.3–0.65 (d_1 is the air hole's diameter of the first layer closest to the core) while d_2/Λ is kept constant at 0.95 (d_2 is the air hole's diameter of the second layer and others). The core of the fibers was completely replaced by composite materials 85% SiO_2-15% GeO_2 with the diameter determined according to the formula $D_c = 2\Lambda - d_1$. By skillfully tuning such lattice parameters, PCF has demonstrated good confinement of light in the core (Fig. 1b).

To design the structures of PCFs, first, the parameters of the refractive index of composite materials 85% SiO_2-15% GeO_2 were calculated according to formula (1–3) [38],[39] and entered into the data system of LMS. Next, the circular lattice is selected from the lattice types data, and the boundary conditions are set up so that the LMS can solve the Maxwell wave equation with minimal loss. The wavelength range investigated is 0.5–2.0 µm which is compatible with existing LMS data.

$$n^2_{SiO_2}(\lambda) = 1 + \frac{0.6961663\lambda^2}{\lambda^2 - 4.679148\times10^{-3}} + \frac{0.4079426\lambda^2}{\lambda^2 - 1.3512063\times10^{-2}} + \frac{0.8974794\lambda^2}{\lambda^2 - 97.93400254} \quad (1)$$

$$n^2_{GeO_2}(\lambda) = 1 + \frac{0.80686642\lambda^2}{\lambda^2 - 4.75722\times10^{-3}} + \frac{0.71815848\lambda^2}{\lambda^2 - 2.3705545\times10^{-2}} + \frac{0.85416831\lambda^2}{\lambda^2 - 140.2313298} \quad (2)$$

$$n^2_{(GeO_2\text{-}SiO_2)}(\lambda) = 1 + \sum_{i=1}^{3} \frac{[SB_i + X(GB_i - SB_i)]\lambda^2}{\lambda^2 - [SC_i + X(GC_i - SC_i)]^2} \quad (3)$$

Where, SB, SC, GB, GC are the Sellmeier confficients for the SiO_2 and GeO_2 glasses, respectively, and X is the mole fraction of GeO_2 (X = 0.15).

Table 1. Sellmeier's coefficients for the GeO_2-doped [39].

Parameters	Values
B_1	0.712771318
B_2	0.454474982
B_3	0.890982737
C_1 (µm)	6.8489546×10^{-2}
C_2 (µm)	1.21900098×10^{-1}
C_3 (µm)	10.1880265

The dependence of the refractive index of pure SiO_2, pure GeO_2, and composite SiO_2-GeO_2 on wavelength is shown in Fig. 2. Pure GeO_2 has the highest refractive index, but PCFs based on it exhibit a large fiber loss [27], so SiO_2 PCFs with a GeO_2 doped core are a good way to think about minimizing the loss. However, this loss increased as the GeO_2 content increased. Therefore, the GeO_2 doping concentration should also be taken into account when designing the structures of PCFs.

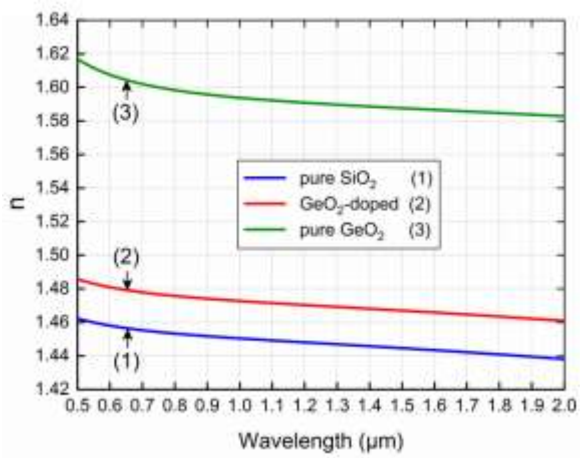

Fig. 2. The real parts of the refractive index *n* pure SiO_2, pure GeO_2, and composite SiO_2-GeO_2.

3. SIMULATION RESULTS AND ANALYSIS

The higher-order modes have a negligible effect on the spectral expansion in SC applications, so the analysis of the optical properties of the PCFs is only for the fundamental mode. Chromatic dispersion is the phenomenon by which different spectral components of a pulse travel at different velocities, which is characterized by the propagation constant β. Chromatic dispersion includes material dispersion and waveguide dispersion. The relationship between dispersion (D) and effective refractive index of the fiber is described in Equation (4) [40].

$$D = -\frac{\lambda}{c}\frac{\partial^2 \mathrm{Re}[n_{\mathrm{eff}}]}{\partial\lambda^2} \tag{4}$$

Where λ and c are the wavelength and the speed of light in a vacuum, respectively, and $\mathrm{Re}[n_{eff}]$ is the real part of the effective index of the guided mode.

The strongly wavelength-dependent dispersion is dominated by structural parameters such as the lattice constant Λ and the filling factor d_1/Λ. Both all-normal and anomalous dispersions are obtained, shown in Fig. 3. In case Λ is small, Λ = 0.9 µm; 1.0 µm, dispersion properties are quite diverse including all-normal and anomalous dispersion curves with one or two ZDWs. When Λ = 0.9 µm (Fig. 3a), there are two all-normal dispersion curves with d_1/Λ = 0.45 and 0.5. The curve with d_1/Λ = 0.45 is closest to the zero-dispersion line in the wavelength range 0.6–1.1 µm, while the one with d_1/Λ = 0.5 is closest to the zero dispersion line in the wavelength range 1.1–2.0 µm. As Λ increases to 1.0 µm (Fig. 3b), the dispersion with d_1/Λ = 0.5 becomes anomalous dispersion with two ZDWs, and d_1/Λ = 0.45 is the flattest all-normal dispersion curve and closest to the zero dispersion curve. With Λ = 1.5 µm and 2.0 µm (Fig. 3c and d), the increase of the filling factor d_1/Λ and Λ causes the dispersion curves to shift upwards, beyond the zero dispersion curve. In this case, we achieve anomalous dispersion for all structures. Furthermore, for Λ = 2.0 µm, the increase of the filling factor d_1/Λ increases the value of the dispersion at each defined wavelength.

The maximum dispersion value is an essential factor to consider the appropriate pump wavelength in SC generation. Usually, the pump wavelengths are chosen close to the peak of the dispersion curves, which also ensures that the corresponding dispersion values are small enough. The change of dispersion maximum value according to the filling factor with different lattice constants is shown in Fig. 4a. For PCFs with small lattice constants (Λ = 0.9, 1.0 µm), the peak of the dispersion curves changes strongly. With the filling factors less than 0.45, these values decrease, reaching a minimum at d_1/Λ = 0.45 and then increasing when d_1/Λ is greater than 0.45. With larger lattice constants (Λ = 1.5, 2.0 µm), the dispersion maximum value increases almost linearly with the increase of the filling factors.

Table 2. The values of ZDWs of the circular SiO_2-GeO_2 PCFs.

$f = d_1/\Lambda$	Λ = 0.9 μm		Λ = 1.0 μm		Λ = 1.5 μm		Λ = 2.0 μm
	ZDW_1	ZDW_2	ZDW_1	ZDW_2	ZDW_1	ZDW_2	ZDW_1
0.3	1.113		1.116		1.022		1.038
0.35	1.237		1.207		0.971		1.011
0.4	1.526		1.498		0.930		0.985
0.45					0.899		0.963
0.5			0.837	1.119	0.874		0.945
0.55	0.810	0.961	0.788	1.164	0.851		0.925
0.6	0.749	1.033	0.752	1.194	0.811		0.910
0.65	0.715	1.060	0.726	1.214	0.813	1.979	0.891

The shift of the ZDWs affects the careful selection of pump wavelengths in the SC generation application, as that relates to the common laser pump wavelengths in practice. Furthermore, the value of dispersion at the pump wavelength must be small enough to improve the SC generation efficiency. Fig. 4b presents the change of ZDWs according to the filling factor d_1/Λ and the values of ZDWs are shown in Tab. 2. For PCFs with small Λ and d_1/Λ, the ZDW_1 value gradually increases (ZDW_1 of the structure Λ = 0.9 μm and d_1/Λ = 0.4 is 1.526), due to the good confinement of light in the small core PCFs. In contrast, ZDW_1 shifts to shorter wavelengths when Λ and d_1/Λ are larger. This suggests that, we can choose the optimal structures with small Λ and d_1/Λ to orient the SC generation application.

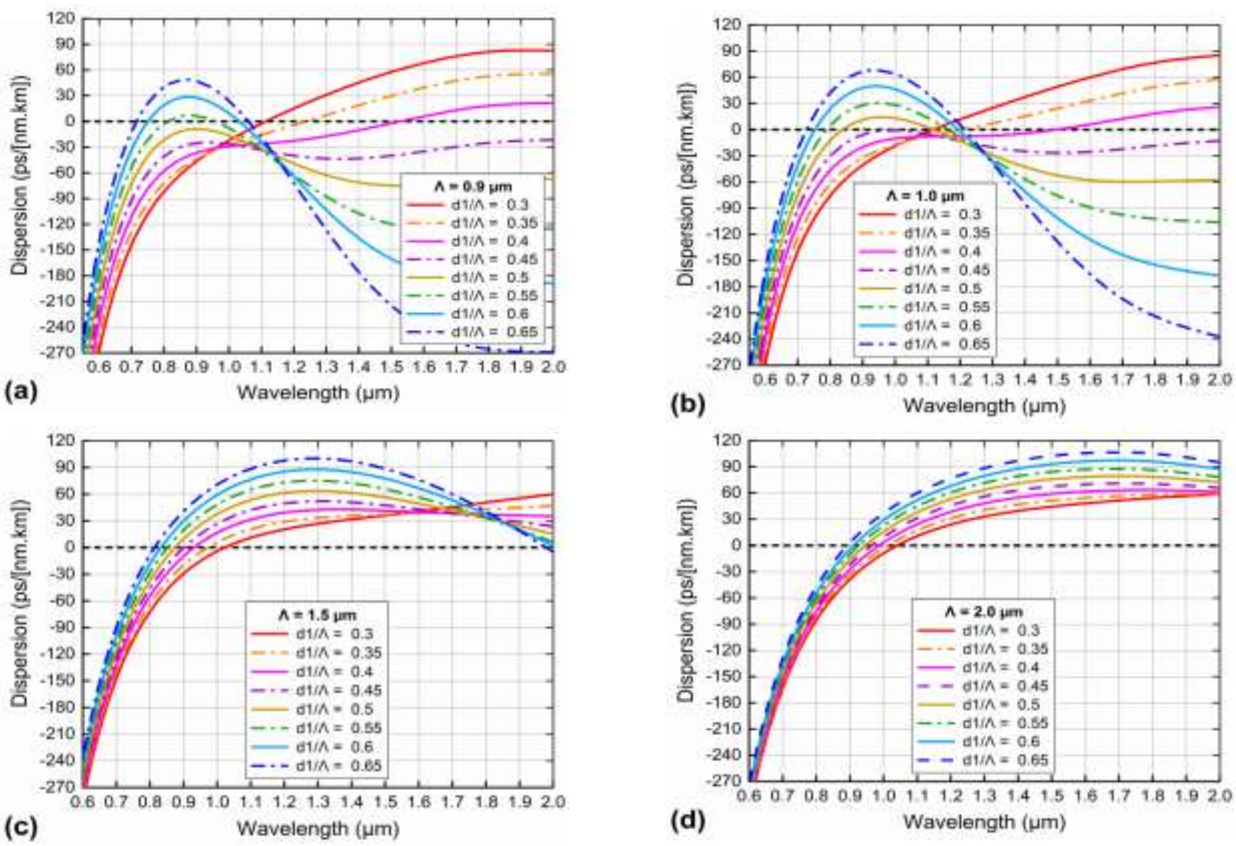

Fig. 3. The chromatic dispersion characteristics of the circular GeO_2-doped silica PCF with various values of d_1/Λ and Λ = 0.9 μm (a), 1.0 μm (b), 1.5 μm (c), and 2.0 μm (d).

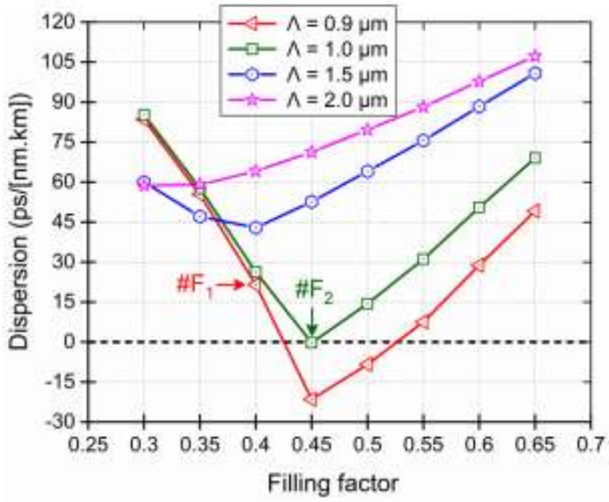

(a) The maximum value of dispersions

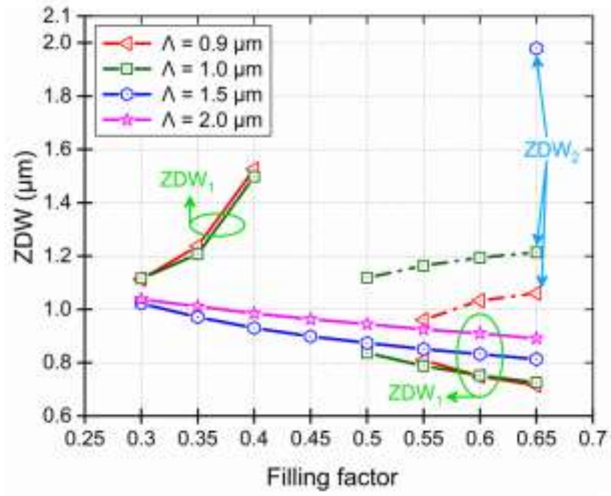

(b) The ZDWs

Fig. 4. The maximum value of dispersions and ZDWs with various filling factors $d1/\Lambda$ and lattice constant Λ

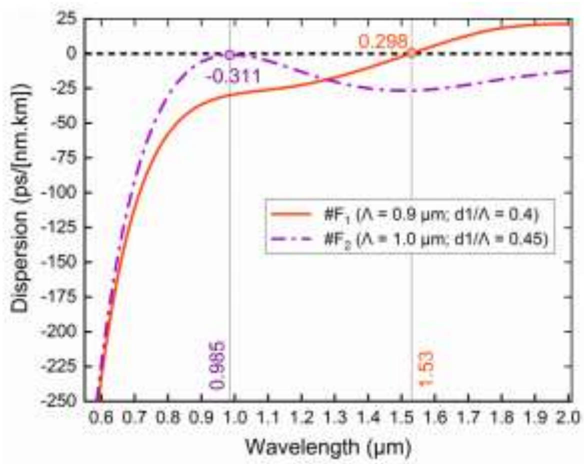

(a) The chromatic dispersion

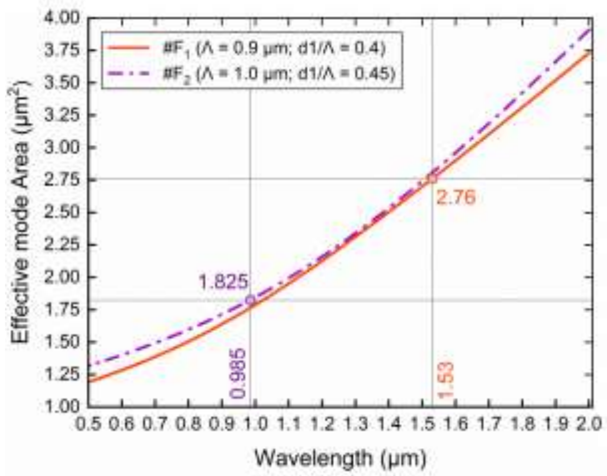

(b) The effective mode area

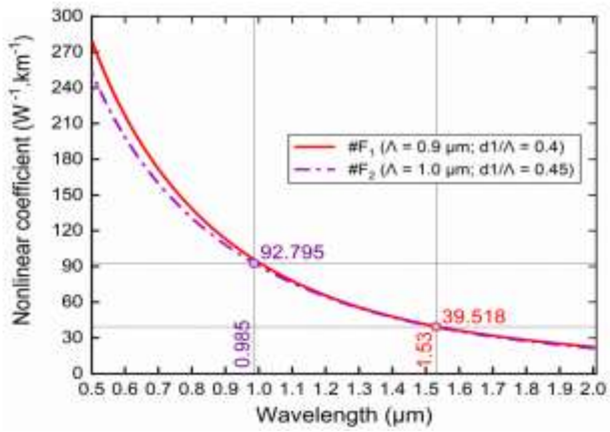

(c) The nonlinear coefficient

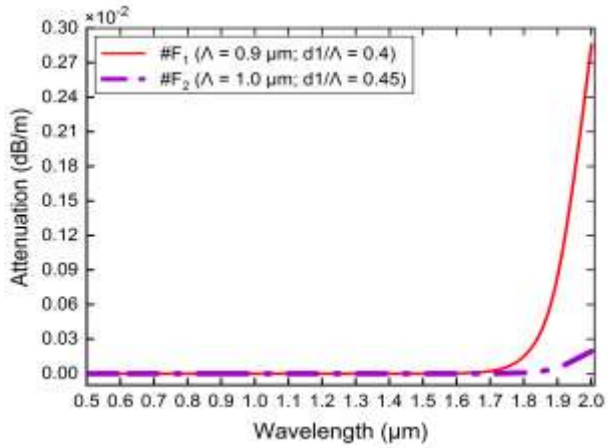

(d) The attenuation

Fig. 5. The optical characteristics of the fundamental mode for #F_1 and #F_2 fibers.

The appearance of different nonlinear effects in SC generation governs the different properties and broadening of the SC spectrum. This strongly depends on the dispersion properties of the proposed PCFs. The broad SC spectrum, high coherence, and low noise are obtained using fiber with all-normal dispersion. For fibers with anomalous dispersion, or a pump wavelength in the anomalous dispersion regime, the SC spectrum is broader but has lower coherence and higher noise. To diversify the applicability of generating SC suitable for the dispersion regime, we propose two PCFs with all-normal and anomalous flat dispersion, named as #F_1 and #F_2 (Fig. 5a). #F_1 fiber with d_1/Λ = 0.4 has the flattest dispersion among anomalous dispersion curves when Λ = 0.9 µm, very small dispersion value of 0.298 ps/nm.km at pump wavelength 1.53 µm (closer to 1.55 µm wavelength of common lasers), is expected to generate a broad and noise SC spectrum with the main mechanism being soliton dynamics. While the #F_2 fiber (d_1/Λ = 0.45 and Λ = 1.0 µm) has normal dispersion with a small dispersion value of −0.311 ps/nm.km at a pump wavelength of 0.985 µm (close to the maximum point of the parabolic dispersion curve) which will give a broad, low noise, and high coherence SC spectrum. Skillfully modifying the structural parameters and choosing a reasonable GeO_2 doping concentration, we obtain a flatter dispersion and the dispersion value at the pump wavelength is smaller than that of the works [25], [28], [42]−[45]. The anomalous dispersion of #F_1 fiber (0.298 ps/nm.km) is about 115 times smaller than the work [44]. Meanwhile, the all-normal dispersion value of #F_2 fiber (−0.311 ps/nm.km) is about 1.8 times, 17 times, and 38 times smaller than the works [25], [32], [43] respectively, but this value is similar to work [28], [41].

Other nonlinear quantities such as effective mode area, nonlinear coefficient, and attenuation of two fibers #F_1 and #F_2 are also investigated in detail. The effective mode area (A_{eff}) is inversely proportional to the nonlinear coefficient (γ) according to the formula (5) [45].

$$\gamma(\lambda) = 2\pi \frac{n_2}{\lambda A_{eff}} \tag{5}$$

Where n_2 is the nonlinear index of the composite (GeO_2-SiO_2).

The dependence of the nonlinear coefficient and effective mode area on the step and structure parameters d_1/Λ , Λ is illustrated in Fig. 5b and c. The increasing wavelength increases the value of A_{eff}, which is consistent with the leakage phenomena of modes out of the core into the cladding of PCFs in the long wavelength region. The A_{eff} of #F_2 fiber is larger than #F_1 in the investigated wavelength range. The large core also increases the leakage of modes resulting in a larger effective mode area. The values of A_{eff} obtained at the pumping wavelength of #F_1 and #F_2 fibers are 2.76 µm^2 and 1.825 µm^2, respectively, which are smaller than [28], [29]. We also achieved a high nonlinear coefficient of 39.518 $W^{-1}.km^{-1}$ and 92.795 $W^{-1}.km^{-1}$ with two fibers #F_1 and #F_2, respectively, which is an advantage in choosing laser pump sources with medium and small peak power. Especially, very low attenuation values (L_k) of about 10^{-8} dB/m of the two proposed fibers are found in the investigated wavelength region, displayed in Fig. 5d. Although the attenuation of both fibers increases sharply at 1.7 µm, it does not affect the SC generation efficiency much because the pump wavelengths of both fibers are lower. Fiber #F_1 has an attenuation value of 3.681×10^{-7} dB/m much larger than fiber #F_2 which is 4.256×10^{-18} dB/m. The structural parameters and values of the proposed two-fiber characteristic quantities are compared with some previous publications on GeO_2-doped silica PCF, manifested in Table 3.

Table 3. The structure parameters and the characteristic quantities of #F_1 and #F_2 fibers at the pump wavelength compared with previous publications on GeO_2-doped silica PCF.

#	% mol GeO_2	D_c (µm)	Λ (µm)	d_1/Λ	Pump wavelength (µm)	A_{eff} (µm^2)	γ ($W^{-1}.km^{-1}$)	D (ps/nm.km)	L_k (dB/m)
#F_1	15	1.44	0.9	0.4	1.53	2.76	39.518	0.298	3.681×10^{-7}
#F_2	15	1.55	1.0	0.45	0.985	1.825	92.795	−0.311	4.256×10^{-18}
[25]	30	-	-	-	1.56	-	-	−5.5	-
	40	-	-	-	1.56	-	-	5	-
[28]	61.8	-	-	-	1.55	3.08	108	−0.322	2.6×10^{-5}
[41]	30	2.8	-	-	1.57	-	11.8	−0.3	0.002
[42]	28.66	-	-	-	1.55	1.96	-	−0.553	0.2×10^{-3}

[43]	4.1	-	-	-	1.55	6.555	13.6	−1.86	-
	7.0	-	-	-	1.55	6.471	14.9	−9.5	-
	13.5	-	-	-	1.55	6.317	16.6	−11.8	-
[44]	-	-	-	-	1.40	7.0	90	34.3	1.12×10^{-10}

4. CONCLUSION

Circular lattice PCFs based on SiO_2-GeO_2 composite (15% mol concentration of GeO_2) are designed with differences in the air hole radius of the layers in the cladding. The modification of lattice parameters including lattice constant and filling factor helps to optimize the dispersion and nonlinear properties of PCFs. We obtain both all-normal and anomalous flat dispersion. Two proposed structures are suitable for SC generation based on a detailed analysis of numerical simulation results. The dispersion values as small as 0.298 ps/nm.km at pump wavelength 1.53 µm are found for fibers $d_1/\Lambda = 0.4$ and $\Lambda = 0.9$ µm with anomalous dispersion. This fiber also shows a nonlinear coefficient as high as 39.518 $W^{-1}.km^{-1}$, and attenuation as low as 3.681×10^{-7} dB/m, which is expected to generate a broad-spectrum SC with soliton dynamics. All-normal dispersion of fibers $d_1/\Lambda = 0.45$ and $\Lambda = 1.0$ µm will produce a highly coherent broad SC spectrum due to the small value of −0.311 ps/nm.km at a pump wavelength of 0.985 µm. With a higher 92.795 $W^{-1}.km^{-1}$ of nonlinear coefficient and a lower of 4.256×10^{-18} dB/m attenuation, this fiber will be suitable for SC generation with small peak power. Two proposed fibers can be a new laser source with low peak power replacing glass core fibers.

REFERENCES

[1] K. Jiao, J. Yao, Z. Zhao, X. Wang, N. Si, X. Wang, P. Chen, Z. Xue, Y. Tian, B. Zhang, P. Zhang, S. Dai, Q. Nie, and R. Wang, **"Mid-infrared flattened supercontinuum generation in all-normal dispersion tellurium chalcogenide fiber,"** *Opt. Express*, 27(3), pp. 2036–2043, 2019. https://doi.org/10.1364/OE.27.002036.

[2] Z. Jiang, T. Wang, Z. Sun, J. Chen, X. Zhang, P. Lin, P. Chen, and Y. Zhao, **"Partially coherent seeding of supercontinuum generation in picosecond regime,"** *Opt. Laser Technol.*, 120, 105752 (5pp), 2019. https://doi.org/10.1016/j.optlastec.2019.105752.

[3] C. Poudel, and C. F. Kaminski, **"Supercontinuum radiation in fluorescence microscopy and biomedical imaging applications,"** *J. Opt. Soc. Am.* B, 36, pp. A139–A153, 2019. https://doi.org/10.1364/JOSAB.36.00A139.

[4] M. Bazargani, B. Gharekhanlou, and M. Banihashemi, **"Improvement in the Transmission Coefficient of Photonic Crystal Power Splitter using Selective Optofluidic Infiltration,"** *Majlesi Journal of Electrical Engineering*, 16(3), 2022, pp. 35–40. https://doi.org/10.30486/mjee.2022.696504.

[5] F. Parandin, and M. M. Karkhanehchi, **"Low Size All Optical XOR and NOT Logic Gates Based on Two-Dimensional Photonic Crystals,"** *Majlesi Journal of Electrical Engineering*, 13(2), pp 1–5, 2019. http://mjee.iaumajlesi.ac.ir/index/index.php/ee/article/view/2703.

[6] F. Borondics, M. Jossent, C. Sandt, L. Lavoute, D. Gaponov, A. Hideur, P. Dumas, and S. Février, **"Supercontinuum-based Fourier transform infrared spectromicroscopy,"** *Optica*, 5, pp. 378–381, 2018. https://doi.org/10.1364/OPTICA.5.000378.

[7] S. Dupont, C. Petersen, J. Thøgersen, C. Agger, O. Bang, and S. R. Keiding, **"IR microscopy utilizing intense supercontinuum light source,"** *Opt. Express*, 20(5), pp. 4887–4892, 2012. https://doi.org/10.1364/OE.20.004887.

[8] M. Seifouri, S. Olyaee, and M. Dekamin, "**A New Design of As_2Se_3 Chalcogenide Glass Photonic Crystal Fiber with Ultra-Flattened Dispersion in Mid-Infrared,"** *Majlesi Journal of Electrical Engineering*, 8(4), pp. 9–15, 2014. http://mjee.iaumajlesi.ac.ir/index/index.php/ee/article/view/1240.

[9] T. N. Thi, D. H. Trong, and L. C. Van, **"Supercontinuum generation in ultra-flattened near-zero dispersion PCF with C_7H_8 infiltration,"** *Opt. Quantum Electron.*, 55, 93, 2023. https://doi.org/10.1007/s11082-022-04351-x.

[10] L. C. Van, T. N. Thi, D. H. Trong, B. T. L. Tran, N. V. T. Minh, T. D. Van, T. L. Canh, Q. H. Dinh, and K. D. Quoc, **"Comparison of supercontinuum spectrum generating by hollow core PCFs filled with nitrobenzene with different lattice types,"** *Opt. Quantum Electron.*, 54(5), 300 (17pp), 2022. https://doi.org/10.1007/s11082-022-03667-y.

[11] T. N. Thi, D. H. Trong, B. T. L. Tran, T. D. Van, L. C. Van, **"Optimization of optical properties of toluene-core photonic crystal fibers with circle lattice for supercontinuum generation,"** *J. Opt.*, 2022. https://doi.org/10.1007/s12596-021-00802-y.

[12] B. T. L. Tran, T. N. Thi, N. V. T. Minh, T. L. Canh, M. L. Van, V. C. Long, K. D. Xuan, and L. C. Van, **"Analysis of dispersion characteristics of solid-core PCFs with different types of lattice in the claddings, infiltrated with ethanol,"** *Photonics Lett. Poland*, 12(4), pp. 106–108, 2020. https://doi.org/10.4302/plp.v12i4.1054.

[13] A. Ghanbari, A. Kashaninia, A. Sadr, and H. Saghaei, **"Supercontinuum generation for optical coherence tomography using magnesium fluoride photonic crystal fiber,"** *Optik*, 140, pp. 545–554, 2017. https://doi.org/10.1016/j.ijleo.2017.04.099.

[14] L. C. Van, H. V. Le, N. D. Nguyen, N. V. T. Minh, Q, H. Dinh, V. T. Hoang, T. N. Thi, and B. C. Van,

"Modelling of lead-bismuth gallate glass ultra-flatted normal dispersion photonic crystal fiber infiltrated with tetrachloroethylene for high coherence mid-infrared supercontinuum generation," *Laser Phys*., 32, 055102 (12pp), 2022. https://doi.org/10.1088/1555-6611/ac599b.

[15] Y. Yang, W. Bi, X. Li, M. Liao, W. Gao, Y. Ohishi, Y. Fang, and Y. Li, **"Ultrabroadband supercontinuum generation through filamentation in a lead fluoride crystal,"** *J. of the Opt. Soc. Am. B*, 36(2), pp. A1-A7, 2019. https://doi.org/10.1364/JOSAB.36.0000A1

[16] Y. Li, L. Wang, M. Liao, L. Zhang, W. Bi, T. Xue, Y. Liu, R. Zhang, and Y. Ohishi, **"Suspended-core fluoride fiber for broadband supercontinuum generation,"** *Opt. Mater.*, 96, 109281 (5pp), 2019. https://doi.org/10.1016/j.optmat.2019.109281.

[17] R. A. H. Ali, M. F. O. Hameed, and S. S. A. Obayya, **"Ultrabroadband supercontinuum generation through photonic crystal fiber шith As_2S_3 chalcogenide core,"** *J. Lightwave Technol.*, 34(23), pp. 5423–5430, 2016. https://doi.org/10.1109/JLT.2016.2615044.

[18] S. Vyas, T. Tanabe, M. Tiwari, and G. Singh, **"Chalcogenide photonic crystal fiber for ultraflat mid-infrared supercontinuum generation,"** *Chin. Opt. Lett.*, 14(12), 123201, 2016. https://doi.org/10.3788/COL201614.123201.

[19] L. C. Van, T. N. Thi, B. T. L. Tran, D. H. Trong, N. V. T. Minh, H. V. Le, and V. T. Hoang, **"Multi-octave supercontinuum generation in As_2Se_3 chalcogenide photonic crystal fiber,"** *Photon. Nanostruct. Fundam. Appl.*, 48, 100986 (10pp), 2022. https://doi.org/10.1016/j.photonics.2021.100986.

[20] A. Medjouri, D. Abed, and Z. Becer, **"Numerical investigation of a broadband coherent supercontinuum generation in $Ga_8Sb_{32}S_{60}$ chalcogenide photonic crystal fiber with all-normal dispersion,"** *Opto-Electronics Review*, 27(1), pp. 1–9, 2019. https://doi.org/10.1016/j.opelre.2019.01.003.

[21] X. Zou, and T. Izumitani, **"Spectroscopic properties and mechanisms of excited state absorption and energy transfer upconversion for Er^{3+}-doped glasses,"** *J. Non-Cryst. Solids*, 162(1–2), pp. 68–80, 1993. https://doi.org/10.1016/0022-3093(93)90742-G.

[22] L. Yang, B. Zhang, K. Yin, J. Yao, G. Liu, and J. Hou, **"0.6-3.2 μm supercontinuum generation in a step-index germania-core fiber using a 4.4 kW peak-power pump laser,"** *Opt. Express*, 24(12), pp. 12600–12606, 2016. https://doi.org/10.1364/OE.24.012600.

[23] D. Jain, R. Sidharthan, P. M. Moselund, S. Yoo, D. Ho, and O. Bang, **"Record power, ultra-broadband supercontinuum source based on highly GeO_2 doped silica fiber,"** *Opt. Express*, 24(23), pp. 26667–26677, 2016. https://doi.org/10.1364/OE.24.026667.

[24] D. Jain, R. Sidharthan, G. Woyessa, P. M. Moselund, P. Bowen, S. Yoo, and O. Bang, **"Scaling power, bandwidth, and efficiency of mid-infrared supercontinuum source based on a GeO_2-doped silica fiber,"** *J. Opt. Soc. Am. B*, 36(2), pp. A86-A92, 2019. https://doi.org/10.1364/JOSAB.36.000A86.

[25] L. Chen, M. Liao, W. Bi, F. Yu, T. Wang, W. Gao, and L. Hu, **"Coherent Supercontinuum Generation in Step-Index Heavily Ge-Doped Silica Fibers With All Normal Dispersion"**, *IEEE Photon. J.*, 14(4), 2022. DOI: 10.1109/JPHOT.2022.3177945.

[26] D. Jain, R. Sidharthan, P. M.Moselund, S. Yoo, D. Ho, and O. Bang, **"High power, ultra-broadband supercontinuum source based on highly GeO_2 doped silica fiber,"** *Fiber Lasers XIV: Technology and Systems*, 10083, 1008318 (4pp), 2017. https://doi.org/10.1117/12.2251648.

[27] P. H. Reddy, A. V. Kir'yanov, A. Dhar, S. Das, D. Dutta, M. Pal, Y. O. Barmenkov, J. A. Minguella-Gallardo, S. K. Bhadra, and M. C. Paul, **"Fabrication of ultra-high numerical aperture GeO_2-doped fiber and its use for broadband supercontinuum generation,"** *Appl. Opt.*, 56(33), pp. 9315–9324, 2017. https://doi.org/10.1364/AO.56.009315.

[28] P. H. Thai, T. T. Pham, Md. A. Hossain, and N. H. Hai, **"A novel design of highly nonlinear golden spiral Ge-doped core photonic crystal fiber for supercontinum light sources application,"** *International Conference on Advanced Technologies for Communications (ATC 2014)*, pp. 681–685, 2014. https://doi.org/10.1109/atc.2014.7043474.

[29] V. A. Kamynin, A. E. Bednyakova, M. P. Fedoruk, I. A. Volkov, K. N. Nishchev, and A. S. Kurkov, **"Supercontinuum generation beyond 2 μm in GeO_2 fiber: comparison of nano- and femtosecond pumping,"** *Laser Phys. Lett.*, 12(6), 065101 (3pp), 2015. https://doi.org/10.088/1612-2011/12/6/065101.

[30] M. Zhang, E. J. Kelleher, T. H. Runcorn, V. M. Mashinsky, O. I. Medvedkov, E. M. Dianov, D. Popa, S. Milana, T. Hasan, Z. Sun, F. Bonaccorso, Z. Jiang, E. Flahaut, B. H. Chapman, A. C. Ferrari, S. V. Popov, and J. R. Taylor, **"Mid-infrared Raman-soliton continuum pumped by a nanotube-mode-locked sub-picosecond Tm-doped MOPFA,"** *Opt. Express*, 21(20), pp. 23261–23271, 2013. https://doi.org/10.1364/OE.21.023261.

[31] V. M. Mashinsky, V. B. Neustruev, V. V. Dvoyrin, S. A. Vasiliev, O. I. Medvedkov, I. A. Bufetov, A. V. Shubin, E. M. Dianov, A. N. Guryanov, V. F. Khopin, and M. Y. Salgansky, **"Germania-glass-core silica-glass-cladding modified chemical-vapor deposition optical fibers: optical losses, photorefractivity, and Raman amplification,"** *Opt. Lett.*, 29(22), pp. 2596–2598, 2004. https://doi.org/10.1364/OL.29.002596.

[32] E. M. Dianov, and V. M. Mashinsky, **"Germania-based core optical fibers,"** *J. Lightwave Technol.*, 23(11), pp. 3500–3508, 2005. https://doi.org/10.1109/JLT.2005.855867.

[33] A. N. Gur'yanov, M. Yu. Salganskii, V. F. Khopin, M. M. Bubnov, and M. E. Likhachev, **"GeO_2-rich low-loss single-mode optical fibers,"** *Inorg. Mater.*, 44(3), pp. 278–284, 2008. https://doi.org/10.1134/S0020168508030126.

[34] D. Jain, R. Sidharthan, P. M. Moselund, S. Yoo, D. Ho, O. Bang, **"High power, ultra-broadband supercontinuum source based on highly GeO2 doped silica fiber,"** Proceedings Vol. 10083, *Fiber Lasers XIV: Technology and Systems* 1008318 2017.

https://doi.org/10.1117/12.2251648.

[35] H. Chen, H. Wei, T. Liu, X. Zhou, P. Yan, Z. Chen, S. Chen, J. Li, J. Hou, Q. Lu, "**All-Fiber-Integrated High-Power Supercontinuum Sources Based on Multi-Core Photonic Crystal Fibers,"** *IEEE Journal of Selected Topics in Quantum Electronics* 20 (5) pp. 64-71 2014. DOI: 10.1109/JPHOT.2011.2175211.

[36] Yang, J., Wang, Y., Fang, Y., Geng, W., Zhao, W., Bao, C., Ren, Y., Wang, Z., Liu, Y., Pan, Z.; et al., **"Over-Two-Octave Supercontinuum Generation of Light-Carrying Orbital Angular Momentum in Germania Doped Ring-Core Fiber,"** *Sensors* 22 6699 2022. https://doi.org/10.3390/s22176699.

[37] J. Cascante-Vinda, S. Torres-Peiró, A. Diez, M.V. Andrés, **"Supercontinuum generation in highly Ge-doped core Y-shaped microstructured optical fiber,"** *Appl Phys B* 98 pp. 371–376 2010. DOI 10.1007/s00340-009-3723-5.19.

[38] I. H. Malitson, **"Interspecimen comparison of the refractive index of fused silica,"** *J. Opt. Soc. Am.*, 55(10), pp. 1205−1208, 1965. https://doi.org/10.1364/JOSA.55.001205.

[39] J. W. Fleming, **"Dispersion in GeO_2-SiO_2 glasses,"** *Appl. Opt.*, 23(24), pp. 4486−4493, 1984. https://doi.org/10.1364/AO.23.004486.

[40] Y. S. Lee, C. G. Lee, F. Bahloul, S. Kim, and K. Oh, **"Simultaneously achieving a large negative dispersion and a high birefringence over Er and Tm dual gain bands in a square lattice photonic crystal fiber,"** *J. Lightwave Technol.*, 37(4), pp. 1254−1263, 2019. https://doi.org/10.1109/JLT.2019.2891756.

[41] J. Liao, Z. Wang, T. Huang, Q. Wei, and D. Li, **"Design of step-index-microstructured hybrid fiber for coherent supercontinuum generation,"** *Optik*, 243, 167393, 2021. https://doi.org/10.1016/j.ijleo.2021.167393.

[42] M. A. Hossain, Y. Namihira, M. A. Islam, and Y. Hirako, **"Polarization maintaining highly nonlinear photonic crystal fiber for supercontinuum generation at 1.55 µm,"** *Opt. Laser Technol.*, 44(5), pp. 1261−1269, 2012. https://doi.org/10.1016/j.optlastec.2011.12.052.

[43] Y. K. Prajapati, V. K. Srivastav, V. Singh, and J. P. Saini, **"Effect of germanium doping on the performance of silica based photonic crystal fiber,"** *Optik*, 155, pp. 149−156, 2018. https://doi.org/10.1016/j.ijleo.2017.10.178.

[44] A. A. Nair, I. S. Amiri, C. S. Boopathi, S. Karthikumar, M. Jayaraju, and P. Yupapina, **"Numerical investigation of co-doped microstructured fiber with two zero dispersion wavelengths,"** Results in Physics, 10, pp. 766−771, 2018. https://doi.org/10.1016/j.rinp.2018.07.032.

[45] G. P. Agrawal**, "Nonlinear Fiber Optics (5th edition),"** *Academic Press, Elsevier*, 2013. https://doi.org/10.1016/C2011-0-00045-5.